JOURNAL OF BACTERIOLOGY, Sept. 1992, p. 5860–5868
0021-9193/92/185860-09$02.00/0

Vol. 174, No. 18

Regulation of the Macrolide-Lincosamide-Streptogramin B Resistance Gene *ermD*

KIM K. HUE AND DAVID H. BECHHOFER*

Department of Biochemistry, Mount Sinai School of Medicine, New York, New York 10029

Received 19 December 1991/Accepted 6 July 1992

The erythromycin resistance gene *ermD*, which encodes an rRNA methylase protein, has an unusually long leader region (354 nucleotides). Previously, a single promoter-proximal leader peptide coding sequence was recognized from the nucleotide sequence, and erythromycin-induced ribosome stalling in this sequence was proposed to be required for the induction of methylase translation. We characterized spontaneously occurring and in vitro-constructed leader region mutations in an effort to understand the function of various segments of the long *ermD* leader region. A second leader peptide coding sequence was identified, and the location of insertion and point mutations that expressed *ermD* methylase constitutively suggested that translation of the second leader peptide is controlled by ribosome stalling in the first leader peptide. From Northern RNA blot analysis of *ermD* transcription, it appears that regulation of *ermD* expression is not by transcriptional attenuation.

Genes that encode inducible resistance to macrolide-lincosamide-streptogramin B antibiotics have been isolated from several gram-positive organisms. These *erm* (erythromycin resistance) genes encode an rRNA methyltransferase (methylase) that methylates a specific residue on 23S rRNA, thereby conferring macrolide-lincosamide-streptogramin B resistance on the host. Methylase expression is induced by subinhibitory concentrations of a subset of macrolide-lincosamide-streptogramin B antibiotics, including erythromycin. A comparison of the sequences of *erm* coding regions shows a high degree of amino acid conservation (8).

The coding regions of inducible *erm* genes are preceded by leader regions of various lengths whose transcription products are predicted to form relatively stable stem-loop structures that function in the regulated expression of these genes. It has been demonstrated conclusively for *ermC* that induction of methylase expression occurs posttranscriptionally (22) by a translational attenuation mechanism (5, 24). In the absence of erythromycin, the ribosome binding site for the *ermC* methylase coding sequence is sequestered by leader region RNA secondary structure. The addition of nanomolar concentrations of erythromycin causes ribosome stalling in a 19-amino-acid coding sequence contained within the leader region (leader peptide coding sequence), which results in destabilization of the leader region RNA stem-loop structure and frees the methylase ribosome binding site and initiation codon for translation. Both *ermA* and *ermG* contain two putative leader peptide sequences, and it has been proposed that a cascade of ribosome stalling is required for induced expression of these methylase genes (19, 20). The promoter-distal 19-amino-acid leader peptides of *ermA* and *ermG* are strikingly similar to the leader peptide of *ermC*, whereas the *ermA* and *ermG* promoter-proximal leader peptide sequences are dissimilar. The putative *erm*(Am) leader peptide consists of 36 amino acids and does not resemble the *ermC* leader peptide (14). It should be noted that direct evidence for leader peptide translation and control of methylase expression by translational attenuation has been obtained only for *ermC* (6, 17, 21).

The present report deals with the leader region of *ermD*, which is 354 nucleotides (nt) in length (12). This is considerably longer than the leader regions of other *erm* genes (*ermC*, 141 nt; *ermG*, 197 nt; *ermA*, 210 nt; *ermAM*, 250 nt), suggesting a more complex form of regulation. The *ermD* leader region sequence appears to be unrelated to that of *ermC*. It has been noted that the *ermD* leader sequence has the potential to fold into different base-paired structures, some of which can account for the sequestering of the methylase ribosome binding site. The *ermD* leader region contains several short open reading frames, only one of which (a promoter-proximal 14-amino-acid coding sequence with no resemblance to other leader peptide sequences) is preceded by a reasonably strong ribosome binding site (LP1 in Fig. 1B). Evidence for posttranscriptional regulation of *ermD* was obtained by showing that inducible expression of *ermD* methylase was not affected when the *ermD* promoter was deleted, such that *ermD* was transcribed from an upstream promoter. In a recent paper (16), Kwak et al. described the cloning and characterization of *ermK*, which has a leader region that differs from the *ermD* leader region at only three nucleotide positions. From their analysis of *ermK* transcription in vivo and in vitro, they concluded that *ermK* methylase expression is regulated by transcriptional attenuation rather than at the translational level. That is, transcription of the full-length *ermK* message is not observed in the absence of induction because of termination of transcription in the leader region. Ribosome stalling in LP1 causes a change in the secondary structure that allows readthrough transcription of the methylase coding sequences.

We isolated and characterized spontaneous deletion, insertion, and point mutations in the *ermD* leader region that express methylase constitutively. We constructed additional mutants to assess the function of various leader region segments. The data presented in this paper indicate that a second leader peptide coding sequence is involved in *ermD* regulation and that control of methylase expression is at the translational level.

* Corresponding author.

MATERIALS AND METHODS

Bacterial strains. All *rec*$^+$ strains were transformants of BD170, which is *trpC2 thr-5*. The *rec* mutant strain was BD224, which is *trpC2 thr-5 recE4*.

Standard procedures. The preparation of *Bacillus subtilis* growth media and competent *B. subtilis* cultures (7), isolation of plasmid DNA (9), oligonucleotide mutagenesis (15), RNA isolation and Northern RNA blot analysis (3, 4), and β-galactosidase assays (12) were as described previously.

Isolation of mutants. The parent *ermD* strain, BG28, containing plasmid pBD244 (Fig. 1A), was chloramphenicol resistant and erythromycin resistant but tylosin sensitive. Spontaneous mutants that grew on tylosin were recovered by growing BG28 overnight in liquid medium containing chloramphenicol (5 μg/ml) and then plating 0.2 ml of a 1:5 dilution of the overnight growth onto solid medium containing 10 μg of tylosin per ml. Colonies that arose after 24 and 48 h of incubation at 34°C were retested for tylosin resistance by streaking on plates containing tylosin at 10 μg/ml. Small-scale plasmid DNA preparations (2) were examined by agarose gel electrophoresis to screen for high-copy-number replication mutants, which confer a tylosin-resistant phenotype, as well as gross plasmid deletions or insertions. Plasmid DNAs that were similar in size to pBD244 were used to transform a *recE4* strain to test for linkage between the chloramphenicol resistance and tylosin resistance markers. A *recE4* strain was used for this purpose because many tylosin-resistant mutants arise due to chromosomal mutations, presumably in ribosomal protein genes, and transformation with DNA isolated by the rapid method contains chromosomal DNA, which could result in transformation to tylosin resistance by recombination. For preparations in which tylosin resistance was demonstrated to be plasmid borne, the plasmid DNA was characterized by digestion with restriction endonuclease *Mbo*I. There are three small *Mbo*I fragments in the *ermD* leader region (125, 65, and 280 bp; Fig. 1A), and small deletions or insertions could be detected by changes in the migration of these fragments in 5% polyacrylamide gels. *ermD* leader regions with mutations were sequenced either by cloning isolated *Mbo*I fragments into the *Bam*HI site of M13mp10 (18) and dideoxy sequencing on single-stranded templates or by amplifying the *ermD* leader region with the polymerase chain reaction and then sequencing the amplified product directly (2).

RESULTS

***ermD* leader region mutations.** To identify elements in the *ermD* 354-nt leader region that are important for regulation of expression, we isolated spontaneously arising mutants that expressed methylase constitutively. A strain carrying the wild-type *ermD* gene on a low-copy-number plasmid cannot grow on 10 μg of tylosin (a noninducing antibiotic) per ml because the basal level of methylase expression is too low to provide resistance. Strains that contain constitutive mutations in the *ermD* leader region can grow on 10 μg of tylosin per ml.

The wild-type *ermD* plasmid pBD244 is shown in Fig. 1A; the strain carrying this plasmid is BG28. As described in Materials and Methods, spontaneously arising Ty^r mutants of BG28 were isolated, and clones in which the Ty^r phenotype was plasmid borne were analyzed further. Plasmids that were similar in copy number and size to pBD244 were examined further. Small insertion and deletion mutants were detected by digestion of plasmid DNA with *Mbo*I, which has three recognition sites in the *ermD* leader region and a fourth site in the proximal coding region (Fig. 1A).

The deletion endpoints in five spontaneously arising deletion mutants (BG42, BG43, BG45, BG47, and BG52) were determined by nucleotide sequencing (Table 1). In BG44, a sixth deletion mutant constructed by Gryczan et al. (12), the *Mbo*I G fragment is deleted. Together, these deletions span most of the *ermD* leader region; this suggests that no segment of the leader region is dispensable for regulation of *ermD* expression. Three small insertion mutants were isolated (BG50, BG51, and BG59; Table 1). Sequencing of the insertion showed that these were duplications of sequences immediately downstream of the previously identified leader peptide coding sequence (LP1). The location of these insertion mutations suggested that this portion of the leader region performs its regulatory function by interacting with the site of predicted ribosome stalling in LP1. This suggestion was strengthened by the isolation of strains with point mutations in nucleotides 144 and 165 (Fig. 1B). Nucleotide 144 is within the LP1 sequence, and the change of TTG to TTC (BG36) or TTG to TTT (BG37) results in a Phe codon instead of a Leu codon at this position. If these changes caused a negative effect on ribosome stalling, the expected phenotype would be noninducible, since, according to the translational attenuation model, ribosome stalling is required for induction of translation. The fact that changes in nt 144 resulted in a constitutive phenotype, and the fact that a mutation at the same position preserved the Leu codon (TTG to TTA; mutant BG41), indicated that the effect of mutations in nt 144 was due to a change in RNA secondary structure rather than to a perturbation of ribosome stalling in LP1. Several clones with mutations in nt 165, which is downstream of the LP1 termination codon, were also isolated (Fig. 1B). In studies on the almost identical *ermK* gene, Kwak et al. (16) also isolated constitutive point mutants that have the equivalent of mutations in nt 144 and nt 165 of *ermD*.

In Fig. 2, a potential hairpin loop structure for this region of the *ermD* leader sequence is presented. Nucleotides 144 and 165 are base paired in this structure, and it could be predicted that the mutations in either nt 144 or nt 165 were affecting this structure. To demonstrate that nt 144 and nt 165 actually formed a base pair, a strain containing reciprocal base changes at these two positions, such that the G-to-C change at nt 144 was present together with a C-to-G change at nt 165 (strain BG65), was constructed. In fact, this strain showed a wild-type inducible phenotype (Table 1), indicating strongly that nt 144 and nt 165 pair in vivo and suggesting that the proposed hairpin structure shown in Fig. 2 may be correct, although this structure could be part of a larger secondary structure. Evidence for an additional secondary structure in this region came from the isolation of a point mutant (BG33) that had an A-to-G change in nt 124. Plate tests indicated that the constitutive Ty^r phenotype of BG33 resulted in tylosin MICs that were lower than those for the strains containing mutations at nt 144 or nt 165 (Table 1). Computer-predicted structures in which the A-to-G mutation in nt 124 destabilizes base pairing between elements in LP1 and LP2 can be drawn. Although the mutation in nt 124 would result in an Arg-to-Gly codon change at this position in LP1, we pointed out above that a negative effect on ribosome stalling should result in a less-inducible phenotype rather than a constitutive phenotype. It should be noted that the constitutive phenotype caused by the mutation in nt 124 would not be predicted by the previously proposed second-

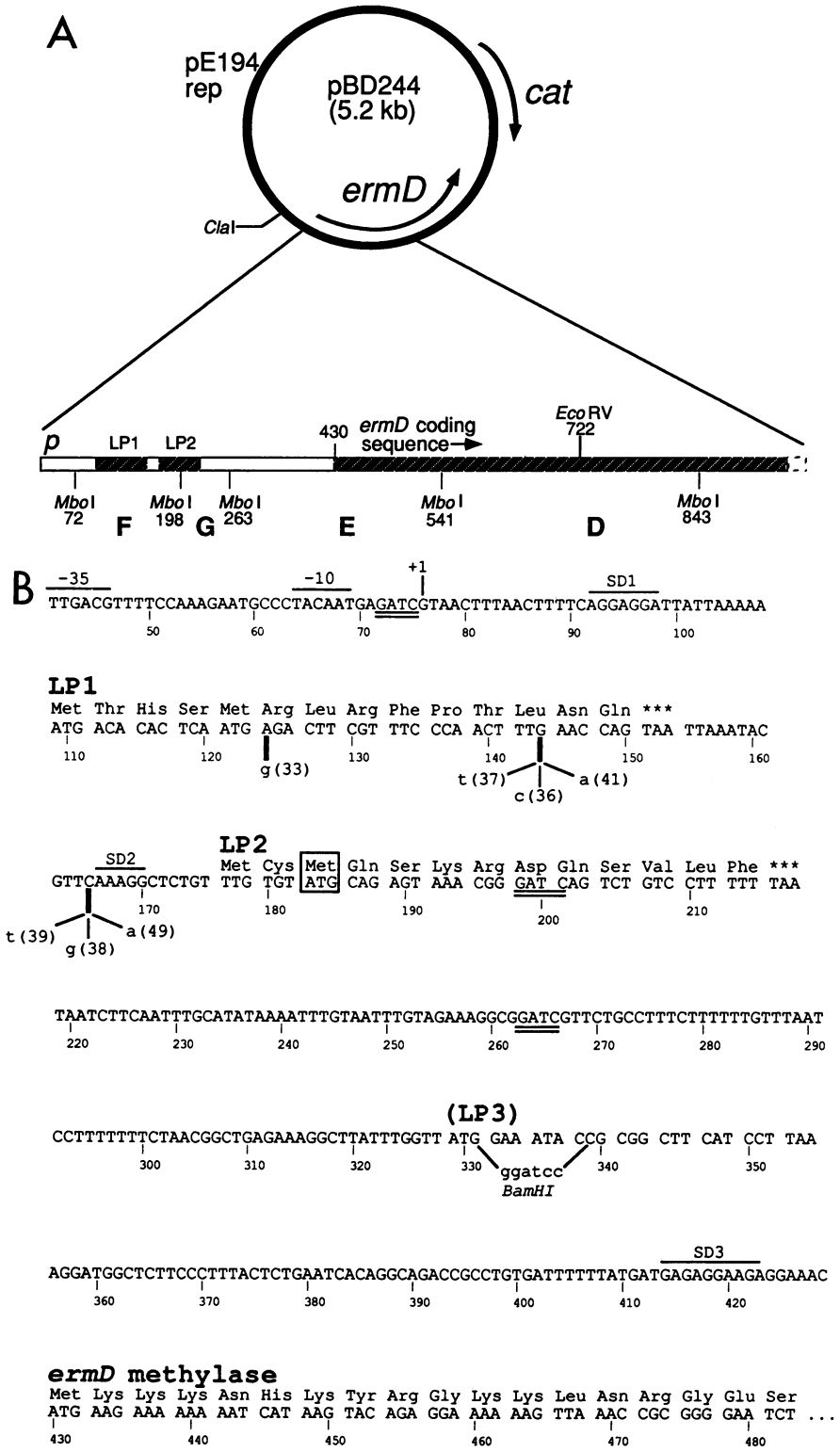

FIG. 1. Structure of plasmid pBD244 and nucleotide sequence of *ermD* leader region. (A) Relative positions of the replication region (pE194rep), chloramphenicol resistance gene (*cat*), and erythromycin resistance gene (*ermD*) are shown on the pBD244 circular plasmid map. A schematic diagram of the *ermD* leader region is shown with the translated portions in dark hatches. The location of the *Mbo*I restriction fragments used to probe *ermD* RNA and the unique *Cla*I and *Eco*RV sites that were used for cloning the *ermD* leader region into *Acc*I-*Sma*I-digested M13mp18 for oligonucleotide mutagenesis experiments are shown. The *Mbo*I fragments labeled F, G, E, and D are the four smallest *Mbo*I fragments of this plasmid. *p*, *ermD* promoter; LP, leader peptide. (B) Nucleotide sequence of *ermD* leader region; the numbering system of Gryczan et al. (11) is used. The location of the *ermD* promoter (−35 and −10), the previously mapped transcription start site (+1), and possible ribosome binding sites (SD) for LP1, LP2, and the methylase coding region are shown. *Mbo*I restriction sites (GATC) are indicated by double underlines. The point mutations at nt 124, 144, and 165 are shown; the substitutions are shown in lowercase letters, followed by the BG number of the strain that carries the mutation. The boxed Met codon at nt 183 was originally thought to be the LP2 initiation codon, but the true initiation codon appears to be the UUG codon at nt 177. The replacement of LP3 codons 2 and 3 to generate a *Bam*HI site is shown in lowercase letters.

TABLE 1. Strains bearing *ermD* leader region mutations

Strain	Type of mutation	nt(s) mutated	Growth on tylosin[a]	Growth on tylosin and erythromycin[a]
BG28	Wild type		−	+
BG42	Deletion	202–266	+++	+++
BG43	Deletion	217–299	++++	++++
BG44	Deletion	83–157	++++	++++
BG45	Deletion	276–339	ND	ND
BG47	Deletion	208–272	+++	+++
BG52	Deletion	80–168	ND	ND
BG50	Duplication	150–188	ND	ND
BG51	Duplication	152–177	+++	+++
BG59	Duplication	152–230	ND	ND
BG33	1 nt	124 (A→G)	+	+
BG36	1 nt	144 (G→C)	++	++
BG37	1 nt	144 (G→T)	ND	ND
BG41	1 nt	144 (G→A)	ND	ND
BG38	1 nt	165 (C→G)	++	++
BG39	1 nt	165 (C→T)	ND	ND
BG49	1 nt	165 (C→A)	ND	ND
BG65	2 nt	144 (G→C) 165 (C→G)	−	+
BG61	Deletion	334, 335, 337 (*Bam*HI site)	+/−−	+
BG62	1 nt	184 (T→A)	−	+
BG63	1 nt	330 (T→A)	+	+
BG66	2 nt	184 (T→A) 330 (T→A)	+/−	+
BG79	1 nt	179 (G→T)	−	+/−−

[a] Growth on solid medium containing either tylosin alone (1.0 μg/ml) or tylosin (1.0 μg/ml) and erythromycin (0.02 μg/ml) was judged by the size of colonies observed after incubation at 33°C for 22 h. −, no growth; +/−−, barely visible colonies; +/−, colonies less than 0.5 mm; +, 0.5- to 1-mm colonies; ++, 1- to 1.5-mm colonies; +++, 1.5- to 2-mm colonies; ++++, 2-mm colonies; ND, plate test not done.

ary structure for this portion of the leader region (16), in which nt 124 is located in a single-stranded bulge.

Northern blot analysis of *ermD* transcription. The initial study on *ermD* regulation (11) showed that deletion of the *ermD* promoter and fusion to an upstream promoter did not affect the inducible phenotype of *ermD* expression, suggesting that regulation was not at the level of transcription initiation. This experiment did not rule out the possibility that regulation was at the level of transcription termination. To assess the transcriptional pattern of *ermD* under inducing and noninducing conditions, a Northern blot analysis (Fig. 3A) was performed on RNA isolated from BG28, the strain containing wild-type *ermD*. Three different single-stranded DNA probes, consisting of *Mbo*I fragments F, E, and D (Fig. 1A) cloned into the *Bam*HI site of M13mp18 or M13mp19, were used. Based on the 5′-end mapping data of Gryczan et al. (11) and their identification of a putative transcription termination sequence, the size of *ermD* mRNA should be about 1,255 nt. The largest band detected in Fig. 3A migrated the same distance as a control 1,260-nt RNA (data not shown). In some experiments the amount of full-length *ermD* mRNA that was detected appeared to increase upon erythromycin induction, but this was not always observed (Fig. 4). It is clear from these experiments that erythromycin induction is not a prerequisite for transcription of full-length *ermD* mRNA.

In the Northern blots shown in Fig. 3A, in addition to the full-length *ermD* mRNA band, two smaller RNA bands migrated at positions that were approximately 200 and 350 nt, based on labeled in vitro-transcribed marker RNAs run in

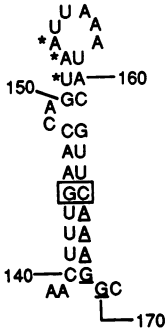

FIG. 2. Potential secondary structure formed by the carboxy-terminal coding sequence of LP1 and the ribosome binding site for LP2. Numbering is as in Fig. 1B. Paired nt 144 and nt 165 are boxed, asterisks mark the termination codon of LP1, and the SD2 sequence is underlined.

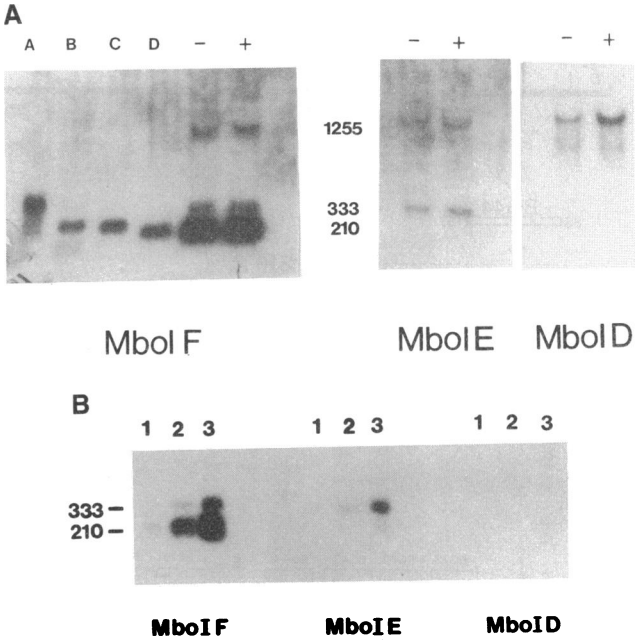

FIG. 3. Northern blot analysis of wild-type *ermD* RNA. (A) RNA isolated from BG28, carrying wild-type *ermD* plasmid pBD244, in the absence of erythromycin (−) or 15 min after the addition of erythromycin (0.02 μg/ml) (+). The RNA was probed with different *Mbo*I single-stranded fragments. The locations of *Mbo*I fragments F, E, and D are shown in Fig. 1A. The numbers next to the detected bands indicate the sizes of full-length *ermD* mRNA (1,255 nt) and smaller RNAs (333-nt and 210-nt RNAs). These sizes are those assigned by Kwak et al. (16) on the basis of their in vitro transcription data. Lanes A through D contained in vitro-transcribed, labeled marker RNAs that were loaded on the gel with 5 μg of total RNA isolated from the parent strain containing no plasmid. The sizes of the markers are 422, 297, 245 and 191 nt in lanes A, B, C, and D, respectively. (B) Equivalent amounts (counts per minute) of the three *Mbo*I fragment probes were used to probe blots containing increasing concentrations of RNA isolated from strain BG28 (lanes): 1, 0.3 μg; 2, 1.2 μg; 3, 6.0 μg. The upstream probe (*Mbo*I-F) detected both the 210-nt and 333-nt RNAs, the middle probe (*Mbo*I-F) detected primarily the 333-nt RNA, and the downstream probe (*Mbo*I-D) detected neither of these RNAs. Only the portion of the blot where the smaller RNAs migrated is shown in panel B.

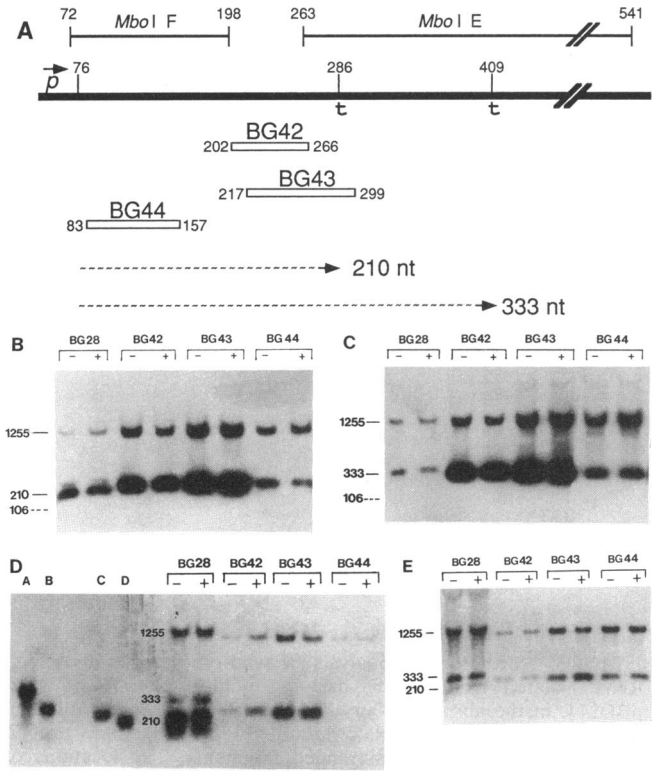

FIG. 4. Northern blot analysis of *ermD* deletion derivatives. (A) Schematic diagram of the *ermD* leader region (■), showing the location of *Mbo*I-F and *Mbo*I-E fragments (——) and the extents of the deletions in strains BG42, BG43, and BG44 (□). Dotted lines show the location of the small RNAs from this region. t, location of potential transcription termination site, as proposed by Kwak et al. (16). (B and C) Northern blots of RNA isolated from *ermD* deletion strains. RNAs were isolated in the absence of erythromycin (−) or 15 min after the addition of erythromycin (+). BG28 carries the wild-type *ermD* plasmid; BG42, BG43, and BG44 carry leader region deletion derivatives (Table 1). Numbers with solid lines on the left of panels B and C indicate the sizes (in nucleotides) of the RNAs detected on the blot. The location of a marker 106-nt in vitro-transcribed RNA that was run in parallel is indicated by the dashed line. This RNA was a control for transfer of small RNA species. The probe for the blot in panel B was the *Mbo*I F fragment, and the probe for the blot in panel C was the *Mbo*I E fragment. (D and E) Northern blots of RNAs isolated from the same strains as in panels B and C, except 1/20 the amount of RNA from the deletion-containing strains was loaded. The probe for the blot in panel D was the *Mbo*I F fragment, and the probe for the blot in panel E was the *Mbo*I E fragment. Markers RNAs in lanes A through D of panel D are the same as those in Fig. 3A. Numbers indicate the sizes (in nucleotides) of *ermD* RNAs.

parallel lanes. To simplify the comparison between our results and those of Kwak et al. (16), we will refer to these two RNAs as the 210-nt and 333-nt RNAs; these predicted sizes are based on the in vitro transcription analysis of Kwak et al. With different probes, the approximate locations of the sequences encoding these RNAs could be determined. The 210-nt and 333-nt bands were detected by the *Mbo*I-F probe, whereas the *Mbo*I-E probe detected primarily the 333-nt band (Fig. 3). There is only a 24-nt overlap between the *Mbo*I-E probe sequence and the predicted 210-nt RNA sequence (see below) (Fig. 4A), which probably explains why the signal for the 210-nt band is weak when the *Mbo*I-E probe is used. The *Mbo*I-D probe, which represents methylase-coding sequences, did not detect either of these two RNAs. If we assume that these RNAs are all transcribed from the *ermD* promoter, the data are consistent with transcription termination occurring at about positions 286 and 409 in the leader region (Fig. 4A), as proposed by Kwak et al., or perhaps processing of the full-length *ermD* RNA occurs at these sites. The synthesis of these small RNAs was also not dependent on erythromycin induction.

To investigate further the nature of these small bands, RNA encoded by plasmids that contained deletions in the *ermD* regulatory region was analyzed by Northern blotting. RNA was isolated from strains BG42, BG43, and BG44 grown with or without erythromycin induction. The positions of these deletions relative to the leader sequence and the proposed RNA products are shown in Fig. 4A. When RNAs isolated from these strains were run in parallel with RNA isolated from the wild-type strain (BG28) and probed with *Mbo*I-F (Fig. 4B) and *Mbo*I-E (Fig. 4C) probes, the lanes containing RNA from the deletion strains gave intense bands that were not in the linear range of the film when the blots were exposed long enough to see the bands in the lanes containing RNA from BG28. Therefore, the Northern blots were repeated with the same amount of total RNA from BG28 but 1/20 the amount of total RNA from the strains containing the deletion plasmids (Fig. 4D and E). The blots were probed with either the *Mbo*I-F probe (Fig. 4D) or the *Mbo*I-E probe (Fig. 4E). The *Mbo*I-E probe detected the full-length RNA and primarily the 333-nt RNA from BG28 as well as the full-length RNA and a smaller band from each of the deletion mutant RNAs. Assuming that the start site for the smaller RNA species in the deletion mutants is the same as the one mapped previously (i.e., at nt 76), then the RNA bands detected by the *Mbo*I-E probe in the BG42 BG43, and BG44 strains should be 268, 250, and 258 nt, respectively. The migration pattern of these RNAs fits well with the predicted sizes. It is important that there appeared to be little difference in the amounts of the full-length RNA and the smaller RNAs in the cultures grown with or without erythromycin.

When the Northern blot of these same RNAs was probed with the *Mbo*I-F probe (Fig. 4D), the full-length 210-nt and 333-nt bands were detected in the BG28 lanes, but the bands detected in the BG42, BG43, and BG44 lanes were the same as those detected by the downstream *Mbo*I-E probe. The expected sizes of deleted versions of the 210-nt RNA would be 145 nt (BG42), 127 nt (BG43), and 135 nt (BG44), but these RNAs were not detected. To control for a possible loss of small RNAs during transfer procedures, uniformly labeled control RNAs that were as small as 106 nt were run on the same blot (Fig. 4B and C). These were readily detectable at all steps in the experiment. It appears, therefore, that although RNAs that are deleted versions of the 333-nt RNA can be detected (with the *Mbo*I-E probe), RNAs that are deleted versions of the 210-nt RNA cannot be detected (with the *Mbo*I-F probe). If the 210-nt RNA arises from transcription termination, it is clear how the deleted RNAs may not be synthesized in the BG42 and BG43 strains, since the deletions in these strains would prevent formation of the transcription terminator structure upstream of position 286. We might expect, however, that the deletion in BG44 would not affect formation of this structure. Our inability to detect a deleted version of the 210-nt RNA in BG44 may be due to the limited region of complementarity (about 40 nt) between the *Mbo*I F probe and the expected RNA, or the deletion in BG44 could somehow also affect termination at position 286.

Potential regulatory elements. Because of the difficulty in explaining how ribosome stalling in LP1 alone could affect translational initiation at the methylase ribosome binding site (SD3), which is located 280 nt downstream of LP1, we examined the leader sequence for other small open reading frames that might contain sites for ribosome stalling. Two additional potential leader peptide sequences (LP2 and LP3 in Fig. 1B), each preceded by a possible Shine-Dalgarno sequence that had limited complementarity to the sequence of the *B. subtilis* rRNA 3′ end, could be recognized. On the basis of the hairpin structure shown in Fig. 2, it seemed reasonable that translation of the putative LP2 could be controlled by ribosome stalling in LP1. That is, in the absence of erythromycin-induced ribosome stalling, the ribosome binding site for LP2 (SD2) would be sequestered, resulting in limited translation of LP2. Ribosome stalling in LP1 would melt the secondary structure shown in Fig. 2 to permit efficient translation of LP2. This arrangement would resemble the cascade of translational events that have been proposed for the regulation of *ermA* and *ermG*, both of which have two potential leader peptide sequences in their regulatory regions. In addition, the constitutive phenotype of the point mutations in nt 144 and nt 165 could be explained by this model, since destabilizing this hairpin would allow translation of LP2 even without ribosome stalling in LP1. Furthermore, the constitutive phenotype of the three insertion mutations, in which SD2 and N-terminal LP2 sequences are duplicated, could be explained, since this duplication would leave the downstream copy of SD2 unpaired and available for translation. Finally, we noticed that a sequence of four amino acids encoded by the putative *ermD* LP2 (codons 3 through 6) was identical to the sequence of codons 5 through 8 in the first leader peptide of *ermG* (Ser, Lys, Arg, Asp [19]).

Testing the role of LP2 and LP3. To test whether potential leader peptide sequences LP2 and LP3 were involved in the regulation of *ermD* expression, the putative initiation codons for LP2 and LP3 were changed from AUG to AAG, a codon that does not function as an initiation codon in bacteria. (At this point, we assumed that the initiation codon for LP2 was the AUG at nt 183 [boxed in Fig. 1B].) Also, the sequence of codons 2, 3, and 4 of LP3 was changed to create a *Bam*HI site, which causes a deletion of codon 3 and changes codon 2 from Glu to Asp. If these potential leader peptide sequences are involved in regulation, we would expect that abolishing or decreasing translation of LP2 or LP3 would result in a noninducible phenotype.

The phenotypes of the strains containing these mutations are shown in Table 1 (strains BG61, BG62, and BG63). The AUG-to-AAG change in the putative LP2 initiation codon (BG62) had no effect on the inducible phenotype, since there was no difference between BG28 and BG62 on plating tests. (Plating tests for the mutants described below were repeated at least three times.) This result suggested that translation of LP2 was not required for the wild-type inducible phenotype (but see below). The AUG-to-AAG change in LP3 (BG63) resulted in the formation of very small colonies on plates containing tylosin, indicating a low-level constitutive phenotype. The changes associated with the introduction of a *Bam*HI site in the LP3 sequence (BG61) caused a slightly constitutive phenotype, as evidenced by the formation of barely visible colonies on plates containing tylosin. In addition, we constructed a strain containing the AUG-to-AAG change in the putative initiation codons for both LP2 and LP3 (BG66). This strain showed tiny colonies on plates containing tylosin; these colonies were intermediate in size between those of BG61 (containing the *Bam*HI site in LP3) and BG63 (containing the AUG-to-AAG change in LP3). On the basis of the slightly constitutive phenotypes of the LP3 mutations, we concluded that changes in the LP3 sequence affected a secondary structure that was required to negatively regulate methylase expression. There was no evidence that translation of either of these potential leader peptides played a role in regulation.

***lacZ* fusions in the *ermD* regulatory region.** To assess directly whether LP3 was being translated, the *Bam*HI site that had been introduced in the LP3 sequence (to give plasmid pED14) was used to fuse the *lacZ* coding region in frame with the putative LP3 coding sequence. *Bam*HI-digested pED14 plasmid DNA was ligated to *Bam*HI-digested pSK10Δ6 (12), which has a *Bam*HI site at codon 8 of *lacZ*. Transformants were plated on solid media containing chloramphenicol (to select for the plasmid) and either no erythromycin or an inducing concentration of erythromycin (0.02 μg/ml). The colonies were screened for β-galactosidase expression by spraying with 4-methylumbelliferyl-β-D-galactopyranoside (25). Among hundreds of nonfluorescing (β-galactosidase-negative) colonies, we noticed one fluorescing (β-galactosidase-positive) colony. Restriction analysis of the leader region DNA from several β-galactosidase-negative clones (and sequence analysis of one sample clone) showed that these were indeed fusions of *lacZ* to LP3. The lack of β-galactosidase expression from this fusion confirmed that LP3 was not being translated. The *ermD* leader region from the lone β-galactosidase-positive clone was sequenced; it contained a fortuitous in-frame fusion of *lacZ* to LP2 that was the result of a deletion from the *Bam*HI site in LP3 to the *Mbo*I site in the middle of the LP2 coding sequence. This deletion recreated a *Bam*HI site, which was used for subsequent constructions. The fact that this fusion gave β-galactosidase expression showed that LP2 was, in fact, being translated. To assess the level of LP2 translation during induction, β-galactosidase expression in cultures grown with or without added erythromycin was assayed with the LP2-*lacZ* fusion strain (BG69) and compared with β-galactosidase expression from a *lacZ* fusion to the *ermD* coding region (BG57) that had been constructed previously (12). The results (Fig. 5) showed a clear induction of β-galactosidase expression with BG57 but high-level constitutive β-galactosidase expression with BG69. (The decrease in the relative amount of β-galactosidase in BG69 over the course of the experiment may be due to instability of the *ermD-lacZ* plasmid carried in this strain. When BG69 and BG57 were grown with chloramphenicol selection and plated on selective media containing 20 μg of methylumbelliferyl-β-D-galactopyranoside per ml, only 20% of the BG69 colonies fluoresced, whereas 95% of the BG57 colonies fluoresced.)

UUG initiation codon for LP2. Since the *lacZ* fusion to LP2 showed that it was indeed translated, the lack of any observable change in the phenotype of strain BG62, in which the putative AUG initiation codon for LP2 had been changed to AAG, suggested that translation initiation was occurring elsewhere. By inspection of the surrounding nucleotide sequence, it seemed possible that the UUG triplet located upstream of the previously mutated AUG codon for LP2 was the true initiation codon for LP2. About 1% of bacterial coding sequences begin with a UUG codon (13). By oligonucleotide mutagenesis, this triplet was changed to UUU, a codon that has not been found to function in vivo as an initiation codon. If translation of LP2 was required for induction of *ermD* expression and the UUG triplet functioned as the initiation codon for LP2, then we would expect

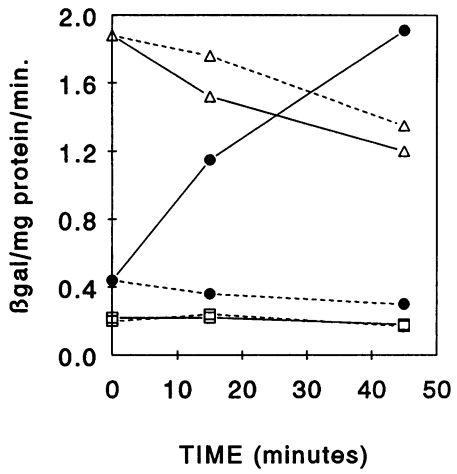

FIG. 5. β-Galactosidase (βgal) expression of *ermD-lacZ* fusions. Aliquots of cultures growing in the absence (- - -) or presence (——) of erythromycin were removed at 0, 15, and 45 min after erythromycin addition and assayed for β-galactosidase activity and total protein. The data represent averages of duplicate samples from one experiment. Similar values were obtained for a repeat of this experiment. Symbols: ●, BG57 (*lacZ* fusion to *ermD* coding sequence; △, BG69 (*lacZ* fusion to wild-type LP2); □, BG78 (*lacZ* fusion to LP2 with mutated UUG initiation codon).

that a change of UUG to UUU would abolish LP2 translation and would result in a noninducible phenotype. In fact, strain BG79, which carried the UUG-to-UUU change, formed barely visible colonies on plates containing tylosin plus an inducing concentration of erythromycin (Table 1). We concluded that translation initiation of LP2 is at the UUG codon and that induction of *ermD* expression is dependent, at least in part, on LP2 translation. In addition, we noted that translation of LP2 from the UUG codon would put the LP2 Ser, Lys, Arg, and Asp codons in the same relative positions that they occupy in the *ermG* LP1 (i.e., codons 5 through 8).

To test directly whether translation of LP2 was affected by the change of the UUG codon at nt 177 to UUU (as in BG79), we took advantage of the *Bam*HI site that had been created by the deletion in BG69 (see above) to create a fusion between the *lacZ* coding sequence and the LP2 sequence with the UUG-to-UUU change (giving strain BG78). β-Galactosidase expression in the presence and absence of erythromycin was measured (Fig. 5). As expected from the noninducibility of BG79 on plate tests (Table 1), no induction of β-galactosidase expression was observed for the fusion to the LP2 sequence with the UUG-to-UUU change (BG78). There was almost a 10-fold difference between the initial β-galactosidase expression in BG69 (wild-type LP2) and that in BG78 (UUG-to-UUU change); this difference can be explained by poor translation initiation at the mutated LP2 initiation codon.

DISCUSSION

The role of specific regions of the 354-nt *ermD* leader region was investigated by analyzing spontaneously arising and in vitro-constructed mutations. Constitutive deletion mutations in which various segments of the leader sequence were missing suggested that all or most of this long leader region is required for the regulation of *ermD* expression. The distance (280 nt) between the end of the promoter-proximal leader peptide coding sequence (LP1) and the methylase-coding sequence suggested either that erythromycin-induced ribosome stalling in LP1 was affecting *ermD* expression by long-range RNA interactions or that there were intervening genetic elements that played a regulatory role. The data presented here indicate that at least one additional leader peptide coding sequence (LP2) is translated and that its translation is required for *ermD* regulation. In particular, the noninducible phenotype of BG79, in which the UUG initiation codon for LP2 was mutated to UUU, shows that translation of LP2 is required for induction of *ermD* expression. Furthermore, the constitutive phenotype of three spontaneously arising insertion mutations that had duplications of the region immediately downstream of LP1 is reminiscent of similar constitutive mutations of *ermC* and *ermA*, whose phenotypes can be explained by obviating the need for ribosome stalling to induce translation of a downstream sequence (10, 20). The distance between LP2 and the ribosome binding site for the methylase coding sequence is 200 nt, which is substantially different from the arrangement of regulatory elements in *ermA* and *ermG*, where only 40 to 45 nt separate the end of the second leader peptide and the ribosome binding site for the methylase coding sequence. It would appear that there is at least one additional regulatory element downstream of LP2. Further experiments will be required to understand the role of leader sequences between LP2 and the methylase coding sequence. In vitro construction of small deletions in this region may help elucidate the function of specific nucleotide sequences.

The relationship between ribosome stalling in LP1 and translation of LP2 could be similar to that proposed for the leader peptide coding sequences in *ermA* (20). That is, the LP2 Shine-Dalgarno sequence (SD2 in Fig. 1B) would be sequestered by the proposed secondary structure for this region (Fig. 2), and erythromycin-induced ribosome stalling in LP1 would melt this structure and allow for translation of LP2. Based on the characteristics of efficient *B. subtilis* ribosome binding sites (1), it would appear that the SD2 sequence is not a very good one, since it has a small polypurine tract of 5 nt (AAAGG) that is surrounded on both sides by short pyrimidine tracts. We might expect that this weak Shine-Dalgarno sequence, combined with the unusual UUG initiation codon, would result in low-level translation of LP2. However, β-galactosidase expression from the LP2-*lacZ* fusion was quite high (Fig. 5). Although it is possible that the translation of LP1 and LP2 is coupled, an analysis of translational coupling in *B. subtilis* (23) suggests that the distance between the stop codon of LP1 and the initiation codon of LP2 is too great to allow efficient coupling. Also, the proposed ribosome stalling in LP1 is not consistent with the idea of translational coupling between LP1 and LP2.

The data from Northern blot analyses of RNA isolated from strains carrying either wild-type *ermD* or deletion mutations in the *ermD* leader region showed that the synthesis of the various RNAs was not dependent on induction. These results must be compared with those obtained by Kwak et al. (16) regarding *ermK*, which has a leader region with only three nucleotide differences from that of *ermD*. These three differences are at positions 129 (G instead of T), 249 (C instead of T), and 344 (A instead of C), and we would not expect these differences to alter the regulatory mechanism substantially. Nevertheless, our analysis of the *ermD*

transcriptional pattern is quite different from that of *ermK*. Although we can detect similar amounts of full-length *ermD* mRNA with or without erythromycin induction, Kwak et al. did not detect a full-length *ermK* message in the absence of erythromycin induction. In addition to the full-length mRNA, two smaller RNAs (210 and 333 nt) were found for both genes. However, although we can readily detect both these RNAs in the absence of induction, the interpretation of the Northern blot analysis of Kwak et al. was that only the 210-nt RNA was present in significant amounts before induction. We cannot explain these apparent discrepancies at present. The only major difference between our Northern blot experiments and those of Kwak et al. was the type of probe used (*Mbo*I fragments cloned into M13 vectors in our case and oligonucleotide probes in the experiments of Kwak et al.), and we would not expect this to yield such differences in the results.

The evidence for transcription termination in the leader region obtained by Kwak et al. is supported by the Northern blot experiments shown in Fig. 4. Specifically, the absence of deleted versions of the 210-nt RNA is consistent with the deletions resulting in the removal of a terminator structure. Although our results concerning the *ermD* RNA products could also be explained by processing of a larger transcript to smaller RNA products, the in vitro transcription data of Kwak et al. exclude this possibility (16). Furthermore, the data in Fig. 4 showed that there was a 10- to 20-fold increase in the steady-state level of small and full-length RNAs in the strains containing deletion mutations. We observed this also with another deletion mutation (data not shown). Removal of transcription termination at position 286 would result in increased transcription of downstream sequences, generating increased amounts of both the 333-nt RNA (or a deleted version thereof) and the full-length mRNA. Finally, the larger amount of the 210-nt RNA that was detected by the *Mbo*I F probe, relative to the amount of 333-nt RNA (Fig. 3A), is also consistent with the 210-nt RNA being generated by transcription termination.

As discussed above, it has been proposed for *ermK* that ribosome stalling in LP1 results in the assumption of an alternate leader region RNA conformation in which the termination of transcription in the leader region is less efficient, thereby allowing transcription of the full-length *ermK* message. Since we observed little difference in the *ermD* transcriptional pattern with and without induction, our data are more consistent with regulation by translational attenuation involving ribosome stalling in LP1 to allow translation of LP2 as well as an additional, as yet undefined, regulatory event. The function of transcription termination in the *ermD* leader region remains to be understood.

ACKNOWLEDGMENTS

The initial part of this work was done in the laboratory of David Dubnau, whom we thank for helpful discussions and a critical reading of the manuscript. The contributions of Jianghao Chen, who isolated BG33, and Peter Komarow, who refined the conditions for isolating Ty^r mutants, are acknowledged.

This work was supported by Public Health Service grant GM-39516 from the National Institutes of Health. The initial work in David Dubnau's laboratory was supported by Public Health Service grant AI-17472 from the National Institutes of Health.

REFERENCES

1. **Band, L., and D. J. Henner.** 1984. *Bacillus subtilis* requires a "stringent" Shine-Dalgarno region for gene expression. DNA **3**:17–21.
2. **Bechhofer, D. H.** 1991. A method for sequencing PCR products can be used to sequence *Bacillus subtilis* "miniprep" plasmid DNA. Biotechniques **10**:17–20.
3. **Bechhofer, D. H., and D. Dubnau.** 1987. Induced mRNA stability in *Bacillus subtilis*. Proc. Natl. Acad. Sci. USA **84**:498–502.
4. **Bechhofer, D. H., and K. Zen.** 1989. Mechanism of erythromycin-induced *ermC* mRNA stability in *Bacillus subtilis*. J. Bacteriol. **171**:5803–5811.
5. **Dubnau, D.** 1984. Translational attenuation: the regulation of bacterial resistance to the macrolide-lincosamide-streptogramin B antibiotics. Crit. Rev. Biochem. **16**:103–132.
6. **Dubnau, D.** 1985. Induction of *ermC* requires translation of the leader peptide. EMBO J. **4**:533–537.
7. **Dubnau, D., and R. Davidoff-Abelson.** 1971. Fate of transforming DNA following uptake by competent *Bacillus subtilis*. I. Formation and properties of the donor-recipient complex. J. Mol. Biol. **56**:209–221.
8. **Dubnau, D., and M. Monod.** 1987. The regulation and evolution of MLS resistance, p. 369–387. *In* Banbury report 24: Antibiotic resistance genes: ecology, transfer, and expression. Cold Spring Harbor Laboratory, Cold Spring Harbor, N.Y.
9. **Gryczan, T. J., S. Contente, and D. Dubnau.** 1978. Characterization of *Staphylococcus aureus* plasmids introduced by transformation into *Bacillus subtilis*. J. Bacteriol. **134**:318–329.
10. **Gryczan, T. J., G. Grandi, J. Hahn, R. Grandi, and D. Dubnau.** 1980. Conformational alteration of mRNA structure and the posttranscriptional regulation of erythromycin-induced drug resistance. Nucleic Acids Res. **8**:6081–6097.
11. **Gryczan, T., M. Israeli-Reches, M. Del Bue, and D. Dubnau.** 1984. DNA sequence and regulation of *ermD*, a macrolide-lincosamide-streptogramin B resistance element from *Bacillus licheniformis*. Mol. Gen. Genet. **194**:349–356.
12. **Gryczan, T. J., M. Israeli-Reches, and D. Dubnau.** 1984. Induction of macrolide-lincosamide-streptogramin B resistance requires ribosomes able to bind inducer. Mol. Gen. Genet. **194**: 357–361.
13. **Gualerzi, C. O., and C. L. Pon.** 1990. Initiation of mRNA translation in prokaryotes. Biochemistry **29**:5881–5889.
14. **Horinouchi, S., W.-H. Byeon, and B. Weisblum.** 1983. A complex attenuator regulates inducible resistance to macrolides, lincosamides, and streptogramin B antibiotics in *Streptococcus sanguis*. J. Bacteriol. **154**:1252–1262.
15. **Kunkel, T. A., J. D. Roberts, and R. A. Zakour.** 1987. Rapid and efficient mutagenesis without phenotypic selection. Methods Enzymol. **154**:367–382.
16. **Kwak, J.-H., E.-C. Choi, and B. Weisblum.** 1991. Transcriptional attenuation control of *ermK*, a macrolide-lincosamide-streptogramin B determinant from *Bacillus licheniformis*. J. Bacteriol. **173**:4725–4735.
17. **Mayford, M., and B. Weisblum.** 1985. Messenger RNA from v*Staphylococcus aureus* that specifies macrolide-lincosamide-streptogramin resistance. Demonstration of its conformations and of the leader peptide it encodes. J. Mol. Biol. **185**:769–780.
18. **Messing, J.** 1983. New M13 vectors for cloning. Methods Enzymol. **101**:10–89.
19. **Monod, M., S. Mohan, and D. Dubnau.** 1987. Cloning and analysis of *ermG*, a new macrolide-lincosamide-streptogramin B resistance element from *Bacillus sphaericus*. J. Bacteriol. **169**: 340–350.
20. **Murphy, E.** 1985. Nucleotide sequence of *ermA*, a macrolide-lincosamide-streptogramin B determinant in *Staphylococcus aureus*. J. Bacteriol. **162**:633–640.
21. **Narayanan, C. S., and D. Dubnau.** 1987. An *in vitro* study of the translational attenuation model of *ermC* regulation. J. Biol. Chem. **262**:1756–1765.
22. **Shivakumar, A. G., J. Hahn, G. Grandi, Y. Kozlov, and D. Dubnau.** 1980. Posttranscriptional regulation of an erythromy-

cin resistance protein specified by plasmid pE194. Proc. Natl. Acad. Sci. USA **77**:3903–3907.
23. **Sprengel, R., B. Reiss, and H. Schaller.** 1985. Translationally coupled initiation of protein synthesis in *Bacillus subtilis*. Nucleic Acids Res. **13**:893–908.
24. **Weisblum, B.** 1983. Inducible resistance to macrolides, lincosamides and streptogramin type B antibiotics: the resistance phenotype, its biological diversity, and structural elements that regulate expression, p. 91–121. *In* J. Beckwith, J. Davies, and J. A. Gallant (ed.), Gene function in prokaryotes. Cold Spring Harbor Laboratory, Cold Spring Harbor, N.Y.
25. **Youngman, P., P. Zuber, J. B. Perkins, K. Sandman, M. Igo, and R. Losick.** 1985. New ways to study developmental genes in spore-forming bacteria. Science **228**:285–291.